DOI: 10.1002/chem.200501025

Unprecedented ROMP Activity of Low-Valent Rhenium–Nitrosyl Complexes: Mechanistic Evaluation of an Electrophilic Olefin Metathesis System

Christian M. Frech,[a] Olivier Blacque,[a] Helmut W. Schmalle,[a] Heinz Berke,*[a] Christian Adlhart,[b] and Peter Chen[b]

Abstract: The reaction of $[Re(H)(NO)_2(PR_3)_2]$ complexes (**1a**: R = PCy_3; **1b**: R = $PiPr_3$) with $[H(OEt_2)_2][BAr^F{}_4]$ ($[BAr^F{}_4]$ = tetrakis{3,5-bis(trifluoromethyl)phenyl}borate) in benzene at room temperature gave the corresponding cations $[Re(NO)_2(PR_3)_2][BAr^F{}_4]$ (**2a** and **2b**). The addition of phenyldiazomethane to benzene solutions of **2a** and **2b** afforded the moderately stable cationic rhenium(I)-benzylidene-dinitrosyl-bis(trialkyl)phosphine complexes **3a** and **3b** as $[BAr^F{}_4]^-$ salts in good yields. The complexes **2a** and **2b** catalyze the ring-opening metathesis polymerization (ROMP) of highly strained nonfunctionalized cyclic olefins to give polymers with relatively high polydispersity indices, high molecular weights and over 80% *Z* configuration of the double bonds in the chain backbone. However, these complexes do not show metathesis activity with acyclic olefins. The benzylidene derivatives **3a** and **3b** are almost inactive in ROMP catalysis with norbornene and in olefin metathesis. NMR experiments gave the first hints of the initial formation of carbene complexes from $[Re(NO)_2(PR_3)_2][BAr^F{}_4]$ (**2a** and **2b**) and norbornene. In a detailed mechanistic study ESI-MS/MS measurements provided further evidence that the carbene formation is initiated by a unique reaction sequence where the cleavage of the strained olefinic bond starts with phosphine migration forming a cyclic ylide–carbene complex, capable of undergoing metathesis with alternating rhenacyclobutane formation and cycloreversion reactions ("ylide" route). However, even at an early stage the ROMP propagation route is expected to merge into an "iminate" route by attack by the ylide function on one of the N_{NO} atoms followed by phosphine oxide elimination. The formation of phosphine oxide was confirmed by NMR spectroscopy. The proposed mechanism is supported further by detailed DFT calculations.

Keywords: density functional calculations · metathesis · reaction mechanisms · rhenium · ring-opening polymerization

Introduction

Transition metal-catalyzed olefin metathesis was discovered in the late 1950s by Eleuterio during investigations with propene over heterogeneous molybdenum catalysts.[1–5] The homogeneous version was first reported in 1967.[6] Since then a variety of applications, such as ring-opening metathesis (ROM), ring-opening metathesis polymerization (ROMP), ring-closing metathesis (RCM), cross metathesis (CM) and acyclic diene-metathesis polymerization (ADMET) have been developed, making olefin metathesis the most widely used C–C bond forming reaction. In particular, the ruthenium-based complexes $[(PR_3)_2Cl_2Ru(carbene)]$[7–10] and $[(PR_3)(NHC)Cl_2Ru(carbene)]$[11–13] (NHC = N-heterocyclic carbene)[14] have broadened the scope of the reaction significantly due to their high activity and excellent tolerance of many common functional groups.[15] The activities of the latter approach the activities of even the very active molybdenum catalysts $[Mo(=CHR)(OR)_2(NAr)]$[16] developed by Schrock. Recently, Piers and co-workers published a fast-initiating 14-electron ruthenium-based catalyst closely related to the Grubbs systems.[17]

[a] Dr. C. M. Frech, Dr. O. Blacque, Dr. H. W. Schmalle, Prof. Dr. H. Berke
Department of Inorganic Chemistry, University of Zürich
8057 Zürich (Switzerland)
Fax: (+41) 44-635-6802
E-mail: hberke@aci.unizh.ch

[b] Dr. C. Adlhart, Prof. Dr. P. Chen
Eidgenössische Technische Hochschule
Laboratorium für Organische Chemie, ETH Hönggerberg
8093 Zürich (Switzerland)

Supporting information for this article is available on the WWW under http://www.chemeurj.org/ or from the author: Cartesian coordinates and computed total bonding energies of optimized geometries.

The mechanism of the olefin metathesis reaction catalyzed by ruthenium–carbene complexes has been the subject of detailed experimental studies,[18–28] including systematic kinetic measurements in solution,[10–13,16–18] gas-phase electrospray ionization tandem mass spectrometry (ESI-MS/MS),[23–26] and X-ray diffraction characterization of model complexes for catalytic intermediates.[10c,27,28] The ligands of the Grubbs-type complexes have a significant impact on initiation rates and on catalyst activities in the reactions of various substrates in solution.[22] Although many efficient catalysts are known, it is still highly desirable to perform screening studies also focussing on the metal center involved.[26,29,30]

Metathesis catalysts based on rhenium, which falls between the highly active Group VI and VIII metals, are mostly heterogeneous.[31] The initiation mechanism of these systems is unknown. However, defined soluble rhenium complexes have rarely exhibited high activity. A few catalysts are known with rhenium in a high oxidation state;[32] systems with rhenium in a low oxidation state have not been studied, except for a dinuclear rhenium–carbonyl complex activated with *i*BuAlCl$_2$.[33,34]

We therefore focused on the development of novel rhenium-based olefin metathesis catalysts. We hoped to combine with this metal center the high activity of the homogeneous molybdenum catalysts and the excellent tolerance to most of the common functional groups found in the ruthenium systems. Our exploration of well-defined [Re(NO)$_2$(phosphine)$_2$]$^+$ cations for use in metathesis catalysis was first triggered by the above-mentioned lack of previous investigations.[35] The high activity of the isoelectronic dinitrosyl–molybdenum and tungsten complexes,[36] for which the catalytically active species is not yet reliably established, but also encouraged our approach.

Results and Discussion

The reaction of the complexes [Re(H)(NO)$_2$(PR$_3$)$_2$] (**1a**: R = PCy$_3$; **1b**: R = P*i*Pr$_3$) with [H(OEt$_2$)$_2$][BAr$^F_4$] ([BAr$^F_4$] = tetrakis{3,5-bis(trifluoromethyl)phenyl}borate) in benzene at room temperature gave the corresponding cations [Re(NO)$_2$(PR$_3$)$_2$]$^+$ (**2a** and **2b**) in very high yields (Scheme 1).[35a,b] Treatment of **2a** and **2b** with phenyldiazomethane in benzene at room temperature led to the moderately stable benzylidene complexes [Re(=CHPh)(NO)$_2$(PR$_3$)$_2$]$^+$ (**3a** and **3b**), isolated in good yields as dark red solids (Scheme 1).

The IR spectra of **3a** and **3b**, particularly the two ν(NO) absorptions, indicate structures possessing two nitrosyl ligands. From the intensities of these bands N-Re-N angles greater than 140° were estimated.[37] These and other structural properties of this type of complex were further supported by an X-ray diffraction study of **3a** crystals obtained by slow crystallization from concentrated methylene chloride solutions at −30 °C. Complex **3a** adopts a pseudo-square pyramidal structure with the phosphine and nitrosyl ligands in the basal positions (Figure 1).[35a] As the P-Re-P and N-Re-N bond angles are very similar (157.97(5) and 156.9(2)°) the square-pyramidal geometry is only slightly distorted. The two bulky *trans*-phosphines are bent away from the carbene, while the nitrosyl ligands, which normally have angles between 111 and 130°, show an open angle here.[35a] The relatively long Re–N bond lengths (1.863(4) and 1.819(4) Å) indicate poorer electron acceptance of the nitrosyl ligands and hence an electronically activated situation. Re–N bond lengths in related dinitrosyl complexes are in the range

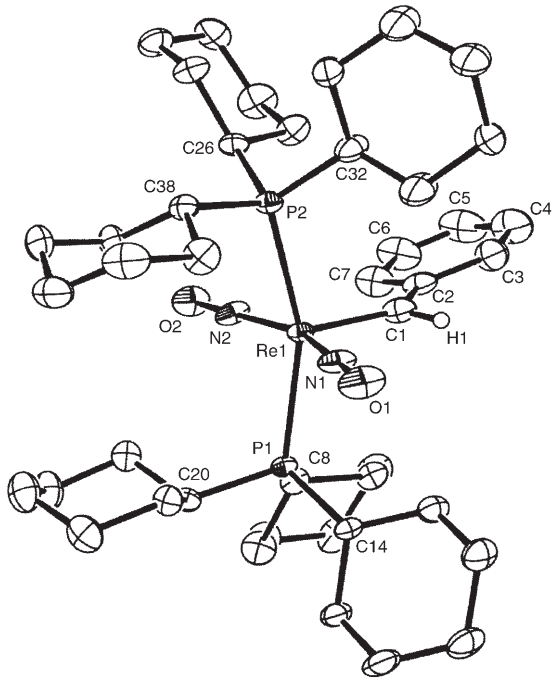

Figure 1. Molecular structure of complex **3a** with thermal ellipsoids at the 30 % probability level (the counter anion [BAr$^F_4$]$^-$ and the hydrogen atoms, except H1, have been omitted for clarity). Selected bond lengths [Å] and angles [°]: Re1–N1 1.863(4), Re1–N2 1.819(4), Re1–C1 1.967(7); N1-Re1-N2 156.9(2), N1-Re1-C1 96.7(3), N2-Re1-C1 106.4(2), P1-Re1-P2 157.97(5).

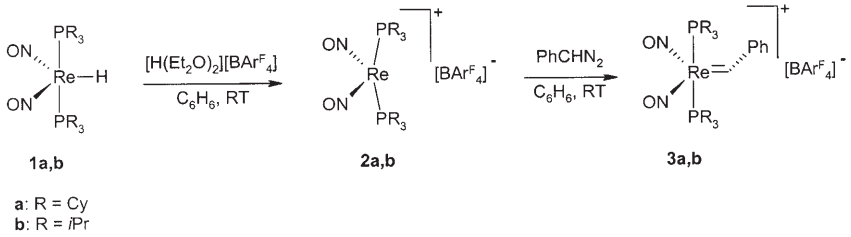

Scheme 1. Synthesis of the benzylidene dinitrosyl bisphosphine cations **3a** and **3b**.

1.72–1.82 Å. Examples are the cationic complexes **2a** and $[Re(CO)(NO)_2(PCy_3)_2]^+$, in which Re–N bond lengths of 1.735(10) and 1.766(8) Å, as well as 1.790(7) and 1.825(5) Å, respectively, have been observed.[35]

Catalytic activity of the isoelectronic dinitrosyl–molybdenum and tungsten complexes has been demonstrated in metathesis reactions,[36] so it was quite surprising that the complexes **3a** and **3b** are almost inactive in olefin metathesis or ROMP. However, this would accord with Schrock's empirical statement that the active species of any olefin metathesis catalyst should be four-coordinated. For **3a** and **3b** this could only be achieved by ligand dissociation from the electronically saturated complexes ($18e^-$), which apparently does not happen. Furthermore, the NO ligands which are not so strongly back-bonding in these cationic systems are not expected to adopt easily the bent bonding mode that would make it possible to circumvent Schrock's requirement.

In exploratory experiments the catalytic ROMP potential of **2a** and **2b** was then tested, assuming that a catalytically active carbene species could eventually be generated from the added olefin similarly to that recently reported in ruthenium(II), osmium(II), and tungsten(0) systems.[38] For heterogeneous Re_2O_7/Al_2O_3 systems and some rhenium complexes in high oxidation states there is a similar situation; it has been proposed that the initial carbene is formed from the olefin by reaction with traces of oxygen, by C–H activation or α-H transfer.[39] An alternative mechanism has been suggested recently.[32] Indeed, the reaction of several strained cyclic olefins, such as norbornene, dicyclopentadiene (DCPD), and cyclooctene, with a 0.1–0.2 % load of the catalysts **2a** or **2b** in chlorobenzene at room temperature, produced polymers of high molecular weight and with a surprisingly high *Z* content of the olefin groups in the polymer backbone (Table 1). The *Z*-olefinic content in ROMP polymers is usually low. Such polymers are usually obtained with tungsten catalysts,[40] but osmium- and ruthenium-based systems have been found to produce *Z*-polynorbornene.[38b,41] The observed relatively high polydispersity indices of the polymers formed may be either a result of a very slow initiation mechanism followed by fast propagation steps, or the consequence of a non-single-site mechanism of the ROMP catalysis, or both.

Table 1. Polymerization of cyclic olefins at room temperature.

Initiator	Monomer	Yield [%][a]	$10^3 M_n$[b]	PDI[c]	*Z* [%][d]	TOF[e]
2a	norbornene	>98	1396	3.945	85	~650
2b	norbornene	>99	1418	2.238	85	~700
2a	DCPD[f]	>97	1085	3.481	–	~650
2b	DCPD[f]	>99	1492	3.626	–	~700
2a	cyclooctene	~20	–	–	75	<100
2b	cyclooctene	~23	2191	1.894	75	<100

[a] Polymerization reactions with norbornene and DCPD were quenched with methanol after 1 h; polymerizations of cyclooctene were quenched after 2 h. [b] Determined by GPC in THF versus polystyrene standards at CIBA Specialty Chemicals, Basel. [c] Polydispersity index M_w/M_n determined at CIBA Specialty Chemicals, Basel. [d] Determined by ^1H and ^{13}C NMR. [e] Turnover frequency in moles of olefin converted per mole of catalyst per hour. [f] DCPD = dicyclopentadiene.

However, it was found that **2a** and **2b** are only suitable catalysts for ROMP of strained and non-heterofunctionalized cyclic olefins. ROMP cannot be accomplished when other strained and functionalized olefins which possess ligating functions are used, presumably because their coordination with unsaturated intermediates is too tight. This was tested for the cyclic olefins such as bicyclo[2.2.1]-5-heptene-2,3-dicarboxylate or 5-norbornene-2-carbonitrile and stresses the necessity for generation of a vacant site, in particular on the initiation pathway. Indeed, the addition of an equimolar amount of a free phosphine or acetonitrile to chlorobenzene solutions of norbornene and **2** resulted in a dramatic decrease in their catalytic activity. When the ROMP reaction mixtures were quenched by treatment with methanol, the polymerization process was stopped immediately. However, it is not clear whether the metal center was released from the polymer or the further coordination of an olefin was prevented just by the presence of methanol.[42] Both chlorobenzene extractions of the polymer and the filtrate did not exhibit catalytic activity after quenching. Remarkably, various acyclic olefins also (for example, 1-hexene, ethyl vinyl ether) did not undergo olefin metathesis in the presence of catalytic amounts of these cations. In order to achieve deeper mechanistic insight into the catalytic ROMP reactions of **2a** and **2b**, the formation of carbene complexes after addition of norbornene to chlorobenzene solutions of **2a** or **2b** was traced by ^1H NMR spectroscopy. In a representative reaction performed with **2a**, several very weak $H_{carbene}$ resonances appeared (δ = 14.62, 13.84, 12.18) in a chemical shift range typical of transition-metal bonding of alkylidenes. We therefore expected the catalytic reaction to have a peculiar and novel initiation mechanism which could not be accessed with acyclic olefins.

Mechanistic studies based on ESI-MS/MS measurements: Further investigations by NMR spectroscopy were not possible because of the small amount of carbene complexes generated, so the transformations of representative olefins with **2b** were studied by electrospray ionization tandem mass spectrometry (ESI-MS/MS).[23,24,43–45] A methylene chloride solution of **2b** was electrosprayed and the mass peak corresponding to the $[Re(NO)_2(PiPr)_3)_2]^+$ cation (*m*/*z* 567) was selected for further collision-induced dissociation (CID) experiments. Suitable collision experiments with norbornene for these studies were not conclusive, most probably because the reactive intermediates generated had the same mass/charge ratio as **2b** or its corresponding norbornene adduct. This assumption was confirmed by using solutions of **2b** and norbornene because no mass peaks were found for characteristic intermediates of the catalytic cycle, even though ROMP polymers were clearly detected in these reaction mixtures. Upon collision with ethyl vinyl ether with low collision energy (~0 eV) at ~8 mTorr a weak peak (*m*/*z* 465) was detected, which was attributed to the 14-electron four-coordinate rhenium–carbene $[Re(=CHOEt)(NO)_2(PiPr_3)]^+$

species **4b**. Formation of the analogous $[Re(=CHOPr)(NO)_2(PiPr_3)]^+$ (*m*/*z* 479; **5b**), as well as two propyl vinyl ether adducts $[Re(NO)_2(PiPr_3)_2(H_2C{=}CHOPr)]^+$ (*m*/*z* 653; **6b**) and $[Re(=CHOPr)(NO)_2(PiPr_3)(H_2CCHOPr)]^+$ (*m*/*z* 565; **7b**) were observed when propyl vinyl ether was used in place of ethyl vinyl ether as CID gas (Scheme 2). The formation of propoxymethylidene complex **5b** supports the interpretation of the previously mentioned peak with *m*/*z* = 465. The mass difference of $\Delta m/z = 14$ between complexes **4b** and **5b** is the same as the mass difference between the two different collision gases applied.

In an independent approach the propyl vinyl ether adduct $[Re(NO)_2(PiPr_3)_2(H_2C{=}CHOPr)]^+$ (**6b**) was generated in the 24-pole, selected upon *m*/*z* (651, ^{185}Re) in Q1, and in a subsequent CID experiment argon was used as the inert collision gas in the octopole. At fairly high collision energies (~27 eV, 0.79 mTorr Ar) loss of propyl vinyl ether was observed predominantly, but a second peak at *m*/*z* = 477 clearly indicated the formation of $[^{185}Re(=CHOPr)(NO)_2(PiPr_3)]^+$ (**5b**) (Figure 2). Furthermore, the mass difference $\Delta m/z$ between adduct **6b** and carbene species **5b** of $\Delta m/z = 174$ is conclusive for mechanistic reasons, because it may be attributed to the loss of the neutral phosphorane $PiPr_3{=}CH_2$, although direct detection of this neutral unit in the mass spectrometer is hampered by the absence of charge.

When the mass (*m*/*z* 465) corresponding to the ethoxymethylene complex $[Re(=CHOEt)(NO)_2(PiPr_3)]^+$ (**4b**) was subjected to ESI MS from the CH_2Cl_2 solution of $[Re(NO)_2(PiPr_3)_2][BAr^F{}_4]$ (**2b**) to which ethyl vinyl ether had been added, and collided with propyl vinyl ether, olefin metathesis reactivity was observed. The formation of the cross-metathesis product $[Re(=CHOPr)(NO)_2(PiPr_3)]^+$ (**5b**) (*m*/*z* 479, ~0 eV, 9 mTorr propyl vinyl ether) and the two adduct peaks $[Re(=CHOEt)(NO)_2(PiPr_3)(H_2C{=}CHOPr)]^+$ (**8b**) and $[Re(=CHOPr)(NO)_2(PiPr_3)(H_2C{=}CHOPr)]^+$ (**7b**) were clearly identified (Scheme 2).

If an ylide $PiPr_3{=}CH_2$ was formed by phosphine migration as indicated by the $[^{185}Re(=CHOPr)(NO)_2(PiPr_3)]^+$ (**5b**) collision experiment with Ar, the formation of the analogous phosphane oxide $(PiPr)_3{=}O$ from the reaction with a carbonyl substrate should be thermodynamically favorable, possibly leading to carbene formation. Thus, $[Re(NO)_2(PiPr_3)_2]^+$ (**2b**) was allowed to collide with benzaldehyde in the CID cell (~7 eV, 2.2 mTorr benzaldehyde). Benzaldehyde adduct **9b**, as well as benzylidene complexes $[Re(=CHPh)(NO)_2(PiPr_3)]^+$ (**11b**) and $[Re(=CHPh)(NO)_2(OPiPr_3)]^+$ (**12b**) formally represented by two peaks at *m*/*z* = 497 and 513 were observed (Scheme 2). The proposed chemical transformation of **9b** into its isomer **10b** is not observable by mass spectrometry but gains support from the

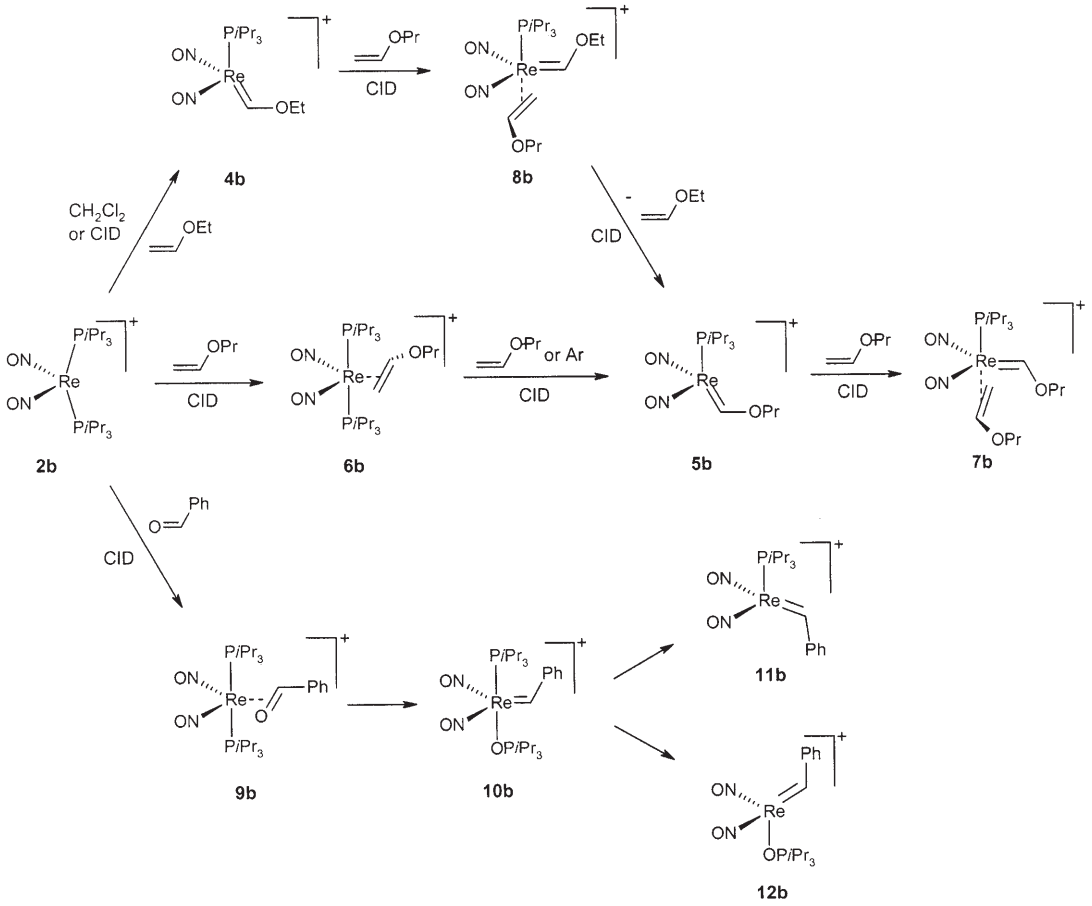

Scheme 2. Observed reactivity of $[Re(NO)_2(PiPr_3)_2]^+$ (**2b**) with vinyl ethers and benzaldehyde in the gas phase and in solution.

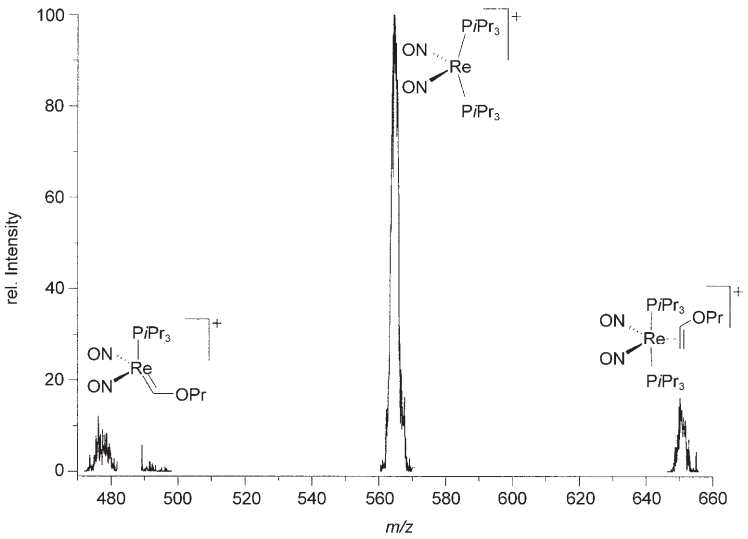

Figure 2. Daughter-ion spectrum of $[^{185}Re(NO)_2(PiPr_3)_2(H_2C{=}CHOPr)]^+$ (**6b**), $m/z = 651$, after collision with Ar in the collision octopole at high energy (nominal 27 eV).

detection of **11b** and **12b**. However, the putative leaving group $PiPr_3{=}O$ corresponding to the $\Delta m/z = 176$ peak again cannot be detected in the gas-phase experiment due to its neutral character. The expected formation of the benzylidene complexes in the gas phase occurs in solution also. Heating of the well characterized complex $[Re(NO)_2(PiPr_3)_2(OCHPh)][BAr^F{}_4]$ (**9b**) to 70 °C in [D5]chlorobenzene led to decomposition of the complex, causing a characteristic proton resonance signal in the NMR spectrum at $\delta = 16.3$ typical of the formation of a rhenium–carbene complex.[35a]

Several gas-phase experiments, collision of **2a** with vinyl ether or with benzaldehyde, or formation of a vinyl ether adduct followed by collision with argon, lead to the formation of a peak which it seems plausible to assign to the same 14-electron carbene species $[Re(=CHR)(NO)_2(PiPr_3)]^+$. The observation of $m/z = 465$ indicates that the rhenium–carbene species $[Re(=CHOEt)(NO)_2(PiPr_3)]^+$ (**4b**) has been formed in the mass spectrometer from the CH_2Cl_2 solution of **2b** containing ethyl vinyl ether. Furthermore, one cross-metathesis step could then be performed in the gas phase with propyl vinyl ether. This suggests that $[Re(=CHR)(NO)_2(PiPr_3)]^+$ is the general propagating species in the gas-phase olefin metathesis after activation of **2b** by acyclic olefins.

The cross-metathesis of a Fischer carbene with vinyl ethers in the gas phase is novel and surprising, as this reaction has not yet been observed for ruthenium–Fischer carbene complexes such as $[RuCl(dcpm)(CHOPr)]^+$.[46] In solution, cross-metathesis of *cis*-propenyl vinyl ether and vinyl butyl ether has been described for $[Cr(CPh_2)(CO)_5]$ where vinyl ethers were obtained as the only products.[47] A related reaction has also been reported recently for Grubbs-type ruthenium–carbene systems.[48]

Analogously to the cross-metathesis experiments of **4b** with propyl vinyl ether, gas-phase reactions of $[Re(=CHOEt)(NO)_2(PiPr_3)]^+$ with norbornene produced the corresponding adduct but no ROMP oligomers were observed. Related experiments with Grubbs catalyst or similar systems led to only low molecular weight oligomers (n up to 6).[49]

Only a few examples are known where Fischer-type carbenes can get involved in ROMP. Thus tungsten complexes are active in ROMP of norbornene at increased temperatures and rhenium compound $[(CO)_5Re{-}Re\{C(OMe)Me\}(CO)_4]$ can be used for olefin metathesis when activated with iBuAlCl2.[34] Formation of Fischer-type ruthenium–carbenes is usually irreversible,[50] and vinyl ethers can even be used to quench ROMP. If in the gas phase $[Re(=CHR)(NO)_2(PiPr_3)]^+$ is the active species in olefin metathesis when $[Re(NO)_2(PiPr)_3)_2]^+$ (**2b**) is used as the initiator, a plausible mechanism of activation remains to be formulated. Further information on this could be obtained from the gas-phase experiment where $[Re(NO)_2(PiPr_3)_2(H_2CCHOPr)]^+$ (**6b**) has been generated in the 24-pole, isolated in the quadrupole, and converted to $[Re(=CHOPr)(NO)_2(PiPr_3)]^+$ **5b** by CID with argon (Figure 2). Because only the isolated adduct complex and energy (by collisions with argon) were available from the CID conditions applied, a general initiation mechanism derived from a simple mass balance can be formulated as represented in Scheme 3.

Initiation of the ROMP reaction of 2a,b with norbornene: Based on the reactivity of the olefin complex **13b** and according to a detailed DFT analysis (see below), an initiation pathway is suggested for the ROMP of norbornene with **2a**,**b**: norbornene is expected first to coordinate with the rhenium center to give **16a**,**b** (Scheme 4). Subsequent mi-

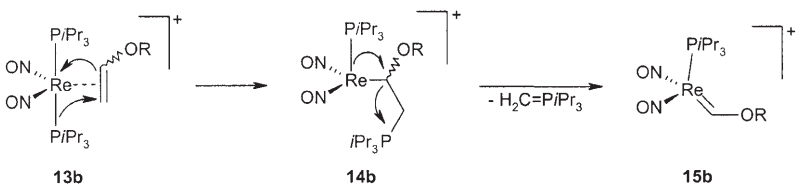

Scheme 3. Suggested initiation mechanism for olefin metathesis by $[Re(NO)_2(PiPr_3)_2(H_2C{=}CHOR)]^+$ (**13b**) in the gas phase.

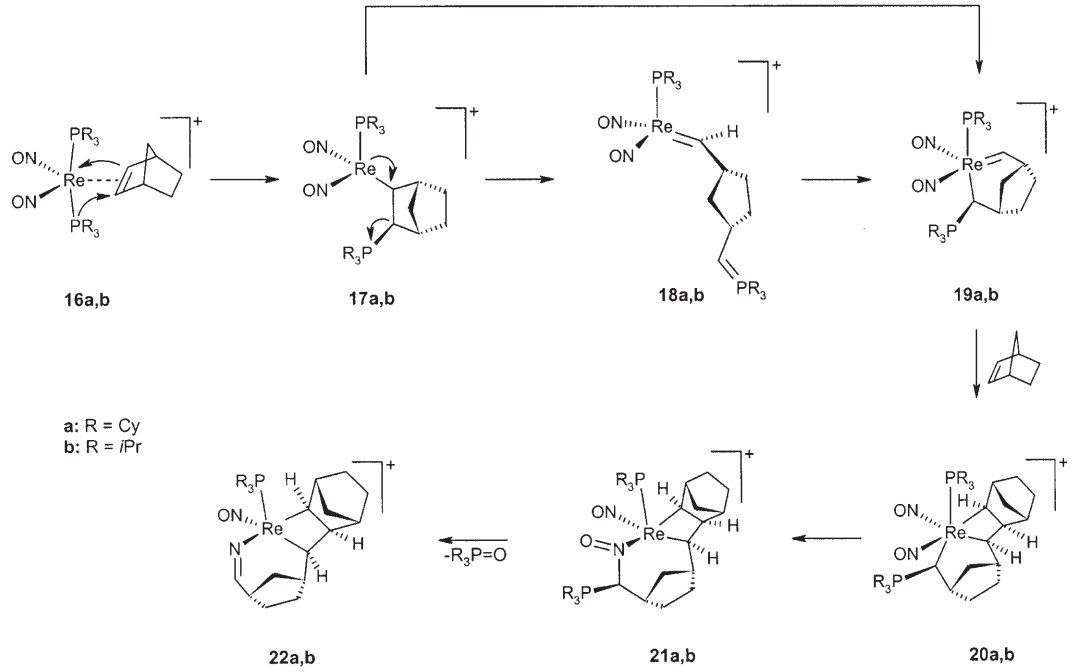

Scheme 4. Suggested initiation pathway for the ROMP of norbornene with **2a**,**b** in solution.

gration of a phosphine to the olefinic moiety yields phosphonio complexes **17a**,**b**, which would then undergo cleavage of the $(C–C)_{norbornyl}$ single bond. A carbene–ylide species **18a**,**b** with a pendant ylide arm is then expected to be formed, which successively coordinates to give **19a**,**b**. It can be envisaged that the intermediacy of **18a**,**b** may be circumvented by a simultaneous process combining the reactions to **18a**,**b** and **19a**,**b**.

The DFT calculations suggest that the formation of the strained alkylidene species **19a**,**b** is at the highest thermodynamic level and their formation is therefore rate determining for the whole ROMP process. Once generated, **19a**,**b** can react further with norbornene, giving the significantly stabilized rhenacyclobutanes **20a**,**b**. Based on this species, subsequent attack of the ylide function on the NO ligand is expected to lead to **21a**,**b**. Thermodynamically favored phosphine oxide elimination would then produce the iminate intermediates **22a**,**b**.

The sequence of initiation steps described gains further support from the thermal behavior of **3a**,**b**: similarly to the formation of **19a**,**b**, a phosphine migration onto a coordinated carbene takes place at 60 °C in chlorobenzene solution, affording the quite stable ylide complexes **23a**,**b** (Scheme 5).

In an X-ray diffraction study the orange-brown complex **23a** was characterized as a $[BAr^F_4]^-$ salt (Figure 3). Complexes of the type **23** and **2** are formally related by their structures and electron counts. Both are cationic $16e^-$ species bearing two NO groups and two $2e^-$ donor ligands. The N-Re-N bond angle (114.2(2)°) of **23a** is indeed similar to that of **2a** (115.9(4)°) but is dramatically reduced compared with that of the $18e^-$ carbene complex **3a** (156.9(2)°). The

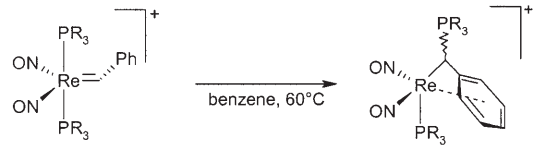

Scheme 5. Synthesis of **23a**,**b** by thermal treatment of **3a**,**b**.

Re–N bond lengths (1.779(4) and 1.758(4) Å) are also shorter than those in **3a**. The narrow Re1-C1-C2 angle of 85.8(3)° supports the idea of a weak interaction between the *ipso* carbon atom (C2) of the phenyl substituent and the rhenium center (Re1–C2 2.531(5) Å) contributing to a partial compensation of the electronic unsaturation of **23a**.

Metathesis propagation cycle starting from 22a,b: Principally three olefin metathesis routes can be envisaged to drive the ROMP metathesis cycle. Denoted as the "ylide", the "C-nitroso", and the "iminate" routes, they start from **20a**,**b**, **21a**,**b**, and **22a**,**b**, respectively. Depending on the thermodynamics, these pathways could even appear as parallel routes. In an alternating fashion rhenacyclobutane and carbene species would be generated with an increasing ring size as the cyclic polymer chain grows (Scheme 6). The "ylide" and "C-nitroso" routes are both at a relatively high thermodynamic level and are therefore expected to merge into the "iminate" route (see the DFT calculations).

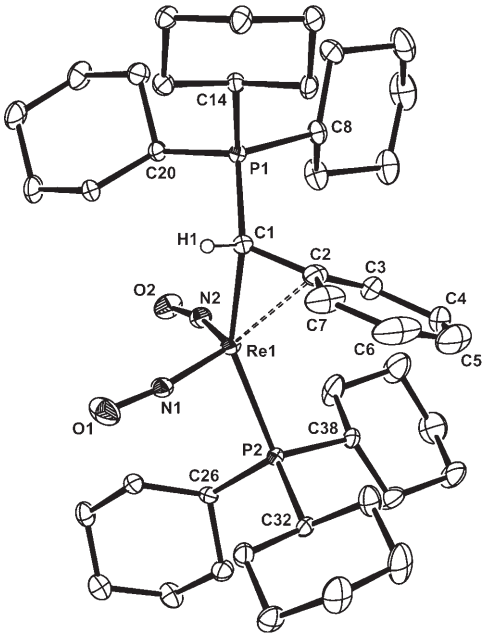

Figure 3. Molecular structure of complex **23a** with thermal ellipsoids at the 30% probability level (the $[BAr^{F}_{4}]^{-}$ counter anion and the hydrogen atoms, except H1, have been omitted for clarity). Selected bond lengths [Å] and angles [°]: Re–N1 1.779(4), Re1–N2 1.758(4), Re1–C1 2.159(5), Re1–C2 2.531(5); N1-Re1-N2 114.2(2), P2-Re1-C1 153.0(1), Re1-C1-P1 126.4(3), Re1-C1-C2 85.8(3).

Species **19a**,**b** and **20a**,**b** of the initiation stage are related to the "ylide" route, but via attack of the ylide function on the NO group and elimination of $iPr_3P{=}O$ or $Cy_3P{=}O$, the "C-nitroso" and the "iminate" routes could subsequently be entered. However, the activation barriers of these steps are not known, so the question of the stage at which the NO attack occurs along the initial "ylide" route is left open. Nevertheless, the DFT analysis suggests that the C-nitroso complex formation could not occur with **19a**,**b**. The ylide rhenacycle formed is presumably at too high a thermodynamic level. The merge into the C-nitroso route could take place, however, at the **20a**,**b** stage or at some other relatively early stages of the propagation pathway. The "C-nitroso" and "iminate" carbene complexes obey Schrock's empirical rule that metathesis carbene complexes have to be four-coordinate and $14e^{-}$ species. With progressive polymer chain buildup, the "iminate" route is assumed to become predominant eventually; in view of the high molecular weights of the polymers this would be relevant for the major part of the polymerization process.

The "C-nitroso" and the "iminate" routes are connected by the thermodynamically favorable formation of phosphine oxide, which was confirmed by NMR spectroscopy in norbornene ROMP experiments with concentrated chlorobenzene solutions of **2a**,**b**. In reference experiments using solutions of **2a**,**b** and norbornane or only **2a**,**b**, phosphine oxide formation was not observed, which confirmed the occurrence of phosphine oxide formation in the initiation/propagation sequence.

Since **19a**,**b** and related higher molecular weight carbene complexes are considered to be key intermediates of the initiation process and the early stages of the propagation of the ROMP catalysis, the question was posed of whether it is possible to mimic these species experimentally. Species **23a**,**b** was treated in situ with phenyldiazomethane, in the expectation that the ylide/benzylidene complexes **24a**,**b** would be generated (see Scheme 7).

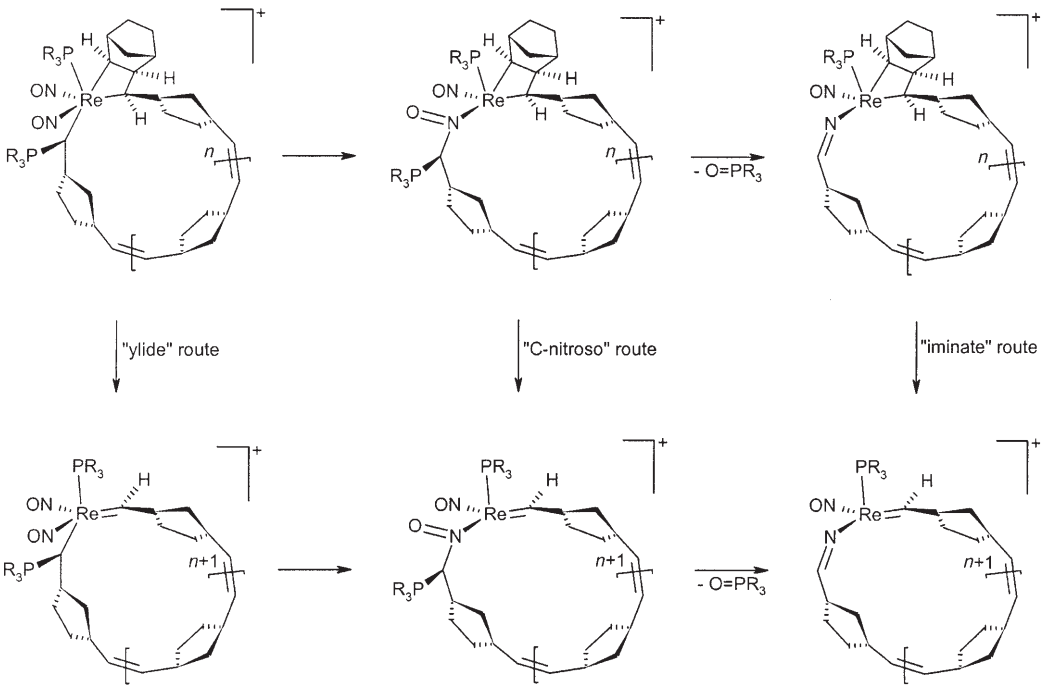

Scheme 6. Possible propagation routes of the ring-opening metathesis polymerization of norbornene.

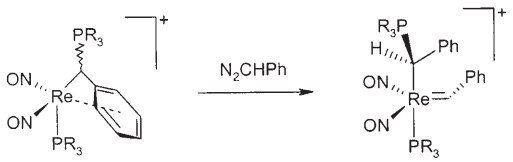

23a,b 24a,b

a: R = Cy
b: R = *i*Pr

Scheme 7. Reaction of **23a**,**b** with phenyldiazomethane.

The ^{1}H NMR spectroscopic analysis of such an experiment using **23a** indeed showed a low-intensity signal at $\delta \sim 16$ indicating the presence of an alkylidene species. Attempts to isolate a pure species of this kind from these reaction mixtures were unsuccessful. Subsequent treatment of the mixtures with norbornene revealed ROMP catalysis of lower activity, but the polymers obtained from these reaction mixtures and norbornene had very similar molecular weights and practically the same *Z*-olefinic content as those polymers obtained from **2a**,**b**. This suggested the presence of related catalytically active centers. In the same way the catalytic activity of **23b** was probed with norbornene. Again catalysis was noticeable with similar polymers revealing a high *Z* content of the backbone olefinic groups.

DFT studies: Since the ROMP mechanisms of complexes **2a** and **2b** could not be fully established on an experimental basis, supporting DFT computational studies were carried out with structural optimization of model intermediates of the ROMP catalysis with norbornene. Attempts to approach crucial transition state geometries failed in the calculation procedure. A related DFT analysis on rhenacyclic systems was performed by Ziegler et al.[51] Scheme 8 shows an extensive ROMP catalysis scheme with various chemically relevant and structurally optimized model intermediates. The DFT calculations were carried out by using PMe_3 ligands and the relative energies are referenced to the total energy of the norbornene complex **16-Me**$^{\perp}$ with an orientation of the olefin perpendicular to the N-Re-N plane. The rotamer with a parallel orientation (**16-Me**$^{\parallel}$) is 4.2 kcal mol^{-1} higher in energy, implying that in complexes **2a**,**b** the olefin ligand may have practically free rotation about the Re–olefin axis at room temperature. A steric influence induced by the phosphine is seen in the Re–C bond lengths of 2.40 Å in the less hindered species **16-Me**$^{\perp}$, about 0.15 Å shorter than for the **16-Me**$^{\parallel}$ isomer (for geometries, see Figure S1 in the Supporting Information). However, in **16-Me**$^{\perp}$ the olefin is indeed in a favorable spatial position for intramolecular phosphine attack. In Scheme 8 the lowest-energy pathway starting from **16-Me**$^{\perp}$ is highlighted and the next species is a phosphonio–norbornyl complex **17-Me** (for geometry, see Figure S2 in the Supporting Information) results. It was calculated to be 12.3 kcal mol^{-1} higher in energy than **16-Me**$^{\perp}$. The optimized structure of **17-Me** shows considerable lengthening of the activated olefinic C–C_{norb} bond, expanding from 1.408 Å in **16-Me**$^{\perp}$ to 1.570 Å and thus preparing for C–C bond rupture.

Cleavage of the olefinic C–C_{norb} bond in **17-Me** could occur yielding the ylide–carbene complex **18-Me** with a pendant ylide function, which would coordinate successively to generate **19-Me**. However, it can be envisaged that a transition state might form more favorably, avoiding loss of rhenium contact of the migrating $C_{norbornene}$ atom and yielding **19-Me** directly (for geometry, see Figure S2 in the Supporting Information). The optimized structures of these complexes have computed energies of +56.0 (**18-Me**) and +31.5 kcal mol^{-1} (**19-Me**) relative to **16-Me**$^{\perp}$. Complex **19-Me** would thus set the highest thermodynamic point on the lowest-energy pathway with highlighted arrows in Scheme 8. [2+2] addition of another norbornene to the Re=C bond of **19-Me**, forming **20-Me**, is slightly exothermic by 5.2 kcal mol^{-1}, while the opening of the rhenacyclobutane leading to **25-Me** (for geometry, see Figure S2 in the Supporting Information) is endothermic by 5.9 kcal mol^{-1}; it has a similar energy to that of **19-Me**. Another norbornene [2+2] addition step was calculated to produce rhenacyclobutane **26-Me**, which was found to be energetically downhill. The dissociation of the PMe_3 ligand *trans* to the ylide unit of **25-Me** to give the 16e$^-$ species **28-Me** would be endothermic by +15.5 kcal mol^{-1}. Complexes related to **28-Me** thus cannot easily be conceived to be intermediates in real catalytic cycles at room temperature.

Starting from **19-Me** the formation of the iminate ligand and the norbornene metathesis along the "C-nitroso" and the "iminate" routes were also explored theoretically. Nucleophilic attack by the ylide ligand on one of the nitrosyl groups to reach the four-coordinated C-nitroso species **29-Me** is energetically uphill by 9.3 kcal mol^{-1}. From **29-Me**, however, a dramatic drop in energy (−36.4 kcal mol^{-1}) would lead in a Wittig-type reaction to the iminate complex **30-Me**. Complex **29-Me**, as well as **30-Me**, could be envisaged to undergo principally norbornene addition, generating the rhenacyclic C-nitroso complex **21-Me** or the iminate complex **22-Me**, respectively. However, in real catalytic systems this route seems unfavorable, since starting from **19-Me** the competing norbornene addition to give **20-Me** would afford a species at lower energy.

The "ylide" propagation route in total represented by the calculated sequence **20-Me**→**25-Me**→**26-Me**→**27-Me** would be "idling" along with a small maximum energy difference of about 6 kcal mol^{-1}, which may be taken as the approximate thermodynamic barrier of the ROMP propagation by using norbornene. Thus structurally related species could appear in the real catalytic systems. However, depending on the activation barriers of the steps **20-Me**→**25-Me** and **26-Me**→**27-Me**, the "ylide" route could eventually merge into the C-nitroso route, at least after a few such steps. The high thermodynamic levels, particularly of species **25-Me** or **26-Me**, makes it quite probable that intramolecular NO attack occurs producing C-nitroso-type intermediates related to **21-Me**, **31-Me**, and **32-Me**. However, **21-Me** is energetically still above the iminate complex **22-Me** by −32.2 kcal mol^{-1}, a

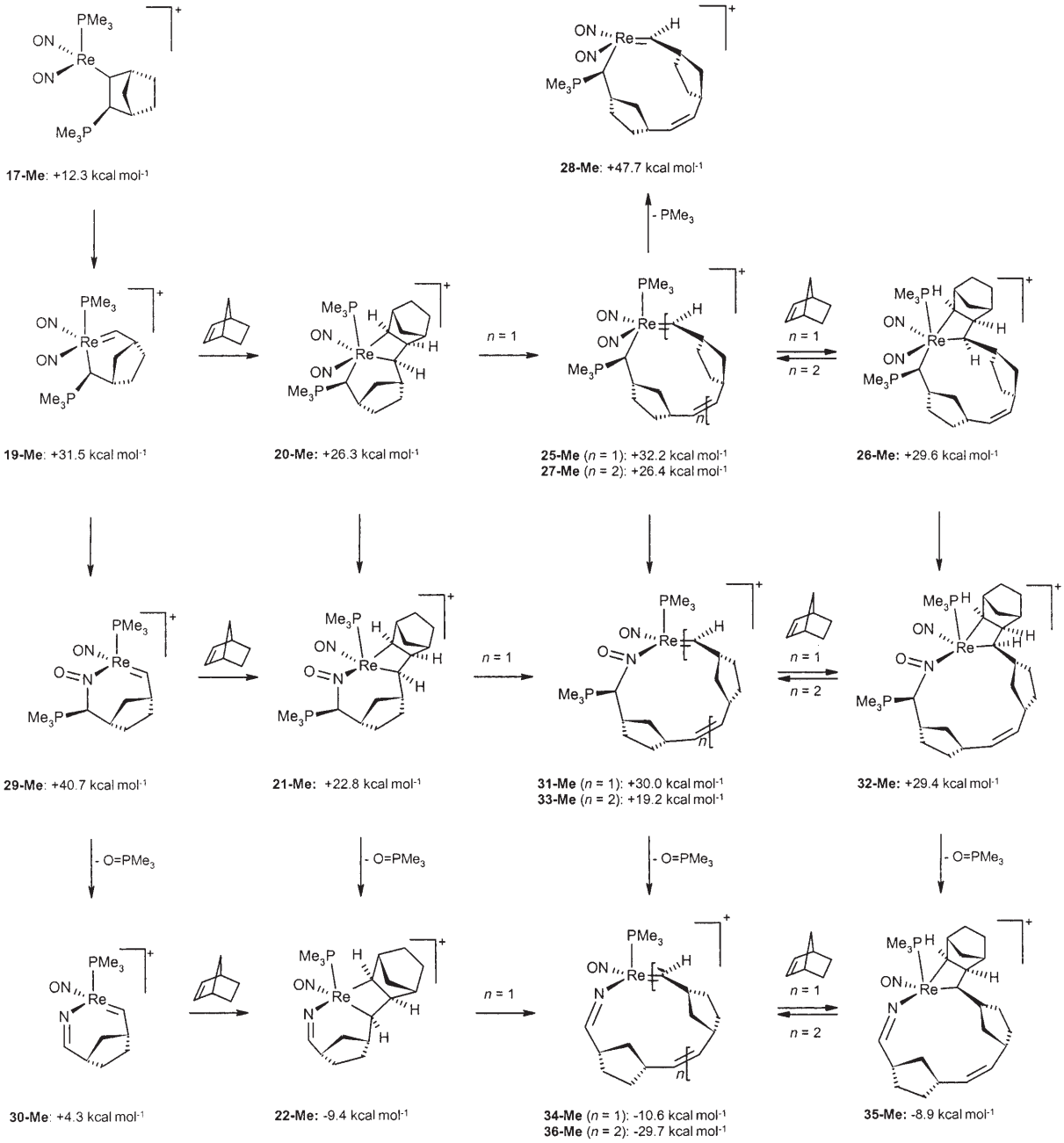

Scheme 8. ROMP catalysis scheme with various chemically relevant and structurally optimized model intermediates.

huge exothermic difference caused by $Me_3P{=}O$ formation. Similar differences exist for the pairs of model complexes **29-Me** and **30-Me**, **31-Me**, and **34-Me** (for geometry, see Figure S2 in the Supporting Information) and **32-Me** and **35-Me**. This makes the "iminate" route a thermodynamic sink, and the most probable to be accessed in real catalytic cycles. Modeling the ROMP propagation of norbornene by the sequence of complexes **22-Me**→**34-Me**→**35-Me** sets lower limits of the barrier for the early "iminate" metathesis sequence. According to this the rhenium–carbene and rhenacyclobutane complexes with the same rhenacycle size are almost on the same thermodynamic level, suggesting that real metathesis systems with norbornene will not be far from being thermoneutral. However, for later stages on the "iminate" route the calculated step of **35-Me**→**36-Me** (for geometry, see Figure S2 in the Supporting Information) would become relevant, which shows a relatively large thermodynamic gain of $-20.8\,\mathrm{kcal\,mol^{-1}}$. This presumably expresses the release of ring strain from the norbornene unit without "compensation" by strain contributions of the iminate ring. All these thermodynamic evaluations suggest that ROMP of norbornene occurs mainly along the "iminate" route.

Stereochemistry of the metathesis reactions: To explain the high *Z* content of the olefinic groups in the polymer chain backbone, the [2+2] additions on the rhenium–carbene species were modeled theoretically along the "iminate" route beyond the molecular sizes of **36-Me**. We tried to picture such attacks of norbornene on the rhenium–carbene species using stereoelectronic rationalizations. First the electronically preferred orientation of a methyl carbene ligand coordinated with the model fragment $[Re(NO)(N{=}CHMe)(PMe_3)]^+$ (**37-Me**) was calculated with prominent rotamers of the open and therefore sterically relaxed iminate complex **37-Me**, which would perhaps help to simulate the electronic preference of high-molecular-weight species (Figure 4).

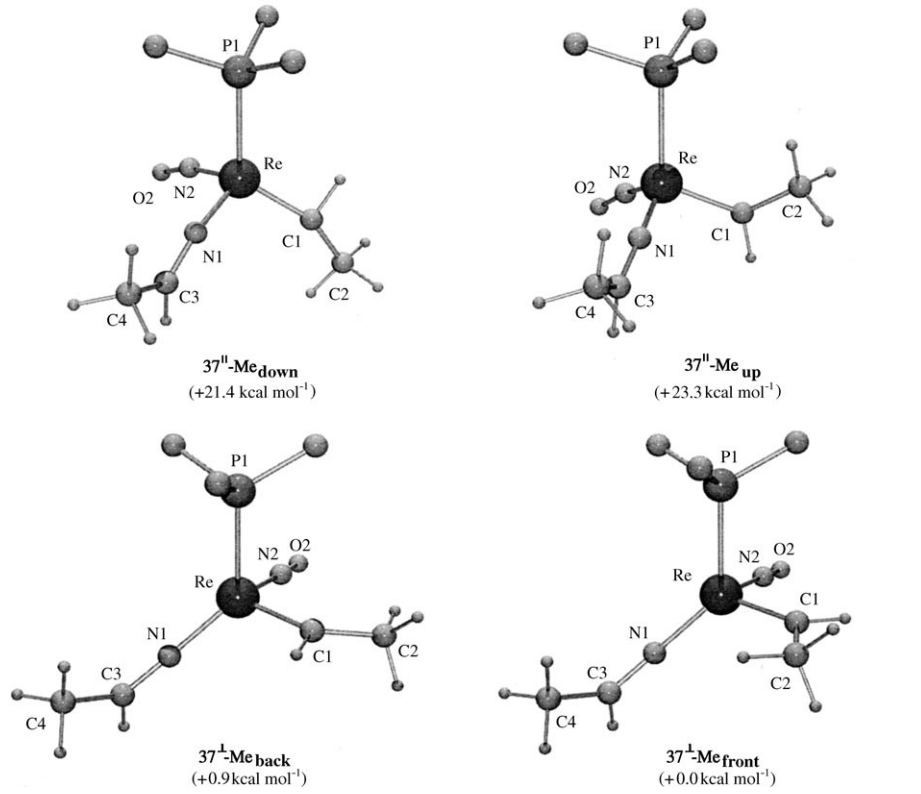

Figure 4. Optimized geometries and relative energies of the model complex **37-Me** with different orientations of the Re=C(Me)H plane. The notation $\parallel$ and $\perp$ refers to orientation relative to the Re–P axis.

For the stereochemical course of the [2+2]-addition steps, the lowest-energy rotamers of **37-Me** are those with the carbene plane oriented perpendicular to the Re–P axis to adopt either the **37**$^{\perp}$**-Me**$_{front}$ or **37**$^{\perp}$**-Me**$_{back}$ conformations. The preferred perpendicular orientation is also in agreement with that of the optimized higher steric demand rotamers of **34-Me** (see Figure 5).

Since the perpendicular orientations of the carbene moieties of both **34-Me** and **37-Me** were calculated to be of considerably lower energies than any parallel orientations, the perpendicular ones are assumed to be the electronically preferred rotamers for the attack of olefins at any stage in the ROMP catalysis of **2a** and **2b** with norbornene. A norbornene attack seems more likely to take place by *exo* approach from below, with the norbornene framework oriented away from the rhenacycle and on the other side of the sterically demanding phosphine, in contrast to attack occurring from above, as Figure 5 may suggest. This assumption of an attack from below is based on the much larger sizes of the real phosphines PCy_3 and $PiPr_3$ in comparison with the model ligand PMe_3. Opening of the rhenacyclobutanes **34**$^{\perp}$**-Me**(ring$_{front}$) and **34**$^{\perp}$**-Me**(ring$_{back}$) (Figure 5) would lead to *E* and *Z* configurations, respectively, in the newly formed olefinic bond. The almost zero energy difference of the back and front orientations of the perpendicular methyl carbene ligand of **37-Me** and the relatively small difference in the comparable orientations of **34**$^{\perp}$**-Me**(ring$_{front}$) and **34**$^{\perp}$**-Me**(ring$_{back}$) suggest that the energy differences of the rotameric carbene species in the actual ROMP catalysis decrease with the release of strain of the iminate carbene ring, that is, with increasing molecular weights of the ROMP intermediates. The supposed presence of initially prevalent isomers related to **34**$^{\perp}$**-Me**(ring$_{front}$) would thus go along with the preference for initial generation of *E* olefinic bonds in the polymeric strands. At a later stage the olefin stereochemistry of the polymers produced could be turned into a preference for *Z*-olefins, when **34**$^{\perp}$**-Me**(ring$_{back}$) species of type could become more and more involved.

Theoretical investigations of metathesis reactions with acyclic olefins: Coordination of ethylene instead of norbornene also gave two minima on the potential energy surface. The two orientations of ethylene (**16′-Me**$^{\parallel,\perp}$) show a smaller total energy difference ($\Delta E = 1.8$ kcal mol^{-1}), however, which demonstrates significant steric influences on the free rotation of the coordinated olefin. Based on the initiation mechanism with phosphine attack on the coordinated olefin and NO attack of the ylide ligand formed, further calculations were sought to evaluate the metathesis path of acyclic olefins using $H_2C{=}CH_2$ as initial reactant in the $[Re(NO)_2(PMe_3)_2]^+$ model system (see Scheme 9). From this study we expected to find out why acyclic olefins do not undergo metathesis in such rhenium–nitrosyl complexes. PMe_3 migration to the ethylene ligand is calculated to be energetically uphill by 12.1 kcal mol^{-1}, but still in a range supposed to be accessible by thermal energy at room temperature. Howev-

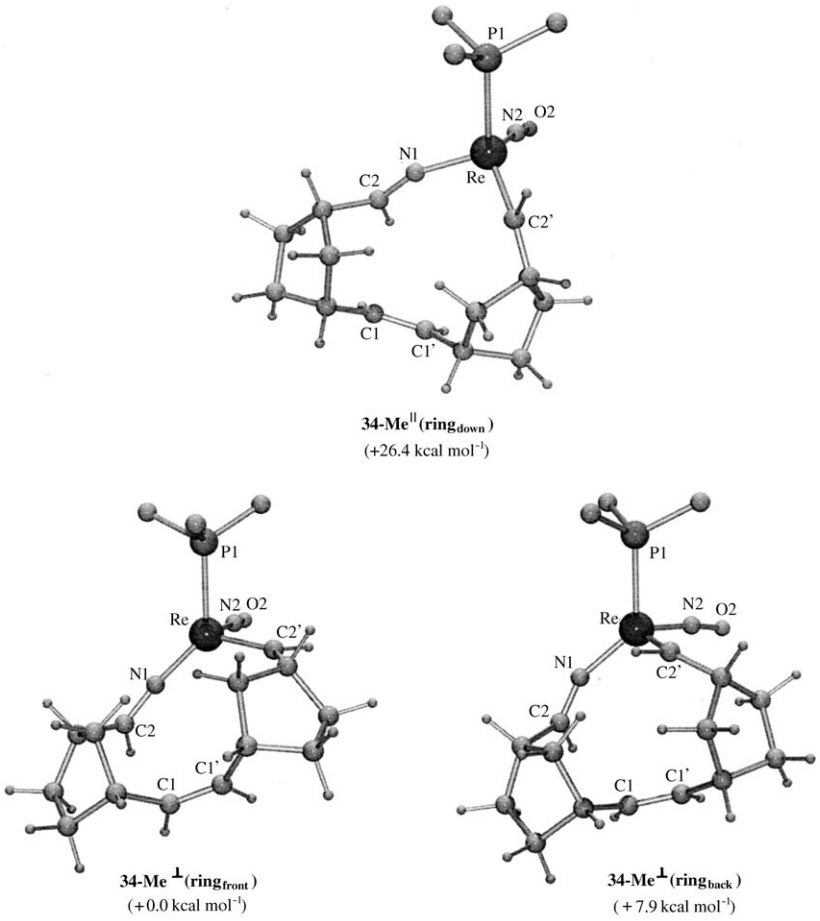

Figure 5. Steric views of prominent carbene rotamers of the model complex **34-Me** in optimized geometries and with relative energies.

er, the formation of the carbene species is calculated to be significantly less favorable for the ethylene species than for the norbornene species ($+24.6$ kcal mol^{-1} for **17′-Me**→**19′-Me**; $+19.1$ kcal mol^{-1} for **17-Me**→**19-Me**), apparently due to the more difficult cleavage of the less activated ethylene double bond.[48] It is the lower thermodynamic stability of the strained olefinic bond in norbornene which eases splitting of the olefinic bond for carbene formation in the initiation phase of ROMP.

The apparent unfeasibility of subsequent conversion of **19′-Me** to **29′-Me** also is related to the absence of a rhenacyclic ring strain. The calculated energy difference between the two molecules is quite large ($+24.3$ kcal mol^{-1}) and **29′-Me** in absolute terms is also at too high an energy with reference to **16′-Me** ($+61.0$ kcal mol^{-1}). Since **19′-Me** is not sufficiently "activated", acyclic olefin metathesis with such systems seems generally incapable of utilizing the NO attack with iminate formation. Furthermore, and in contrast to the related reaction of norbornene, formation of the rhenacyclobutane species **20′-Me** appears energetically downhill by -15.1 kcal mol^{-1} with respect to **19′-Me**. The re-opening of the rhenacycle of structures like **20′-Me** would be too greatly hindered energetically, which might constitute a second reason for the inactivity of **2a**,**b** in acyclic olefin metathesis. In total these theoretically derived factors would indeed account for the experimental observation that only strained cyclic olefins can be involved in metathesis reactions. One can predict that the only acyclic

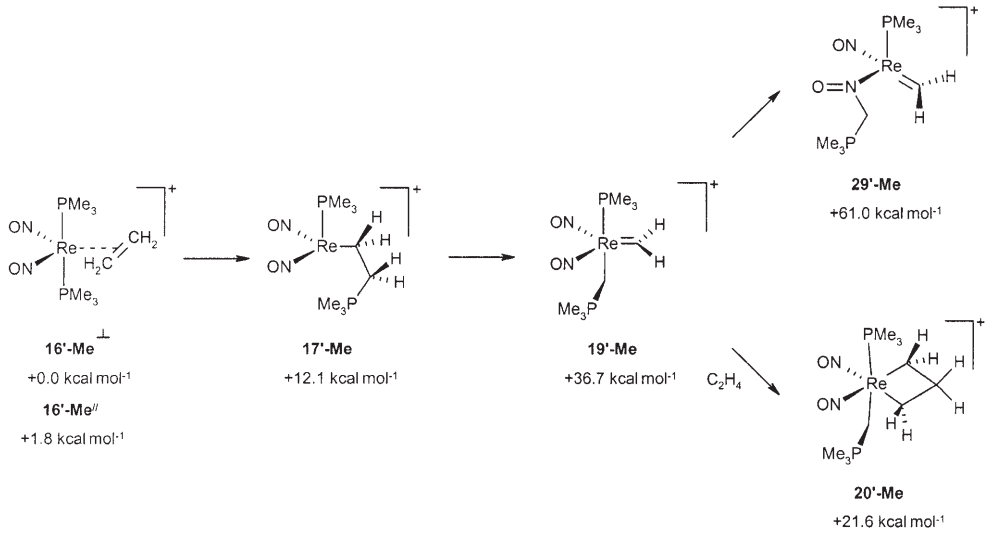

Scheme 9. Metathesis path of acyclic olefins using ethylene as initial reactant with chemically relevant and structurally optimized model intermediates.

olefins that can undergo the initiation sequence of steps are those which have activated structures of type **19**, and which for the propagation sequence would possess specific substitution patterns causing destabilization of the metallacyclobutane structures.

Conclusion

We report here the unprecedented catalytic activity of novel cationic low-valent rhenium-based dinitrosyl–bisphosphine–rhenium complexes in ROMP reactions. The catalytic activity of these 16-electron complexes was unprecedented, since no carbene ligand is present a priori and none of their ligands can be envisaged to be converted into a carbene unit. The formation of a carbene ligand is accomplished in situ by reaction with highly strained, non-functionalized cyclic olefins, such as norbornene. No metathesis activity is observed for simple olefins. The mechanism presented is supported by experimental and theoretical studies and involves the cleavage of the strained olefinic bond by phosphine migration forming an ylide–carbene complex. The intramolecular reaction of the ylide function with a nitrosyl ligand leads in a Wittig-type reaction to elimination of phosphine oxide as a key step, and provides a high thermodynamic driving force in the initial course of reaction. The initial "ylide" route thus merges into the "iminate" route, by which the major part of propagation of the ROMP polymerization may proceed. The initiation mechanism presented here may exist generally in the realm of electrophilic olefin metathesis systems.

Experimental Section

General: All synthetic operations were conducted in oven-dried glassware using a combination of glove-box (M. Braun 150B-G-II), high-vacuum, and Schlenk techniques under a dinitrogen atmosphere. Solvents were freshly distilled under N_2 by standard procedures and were degassed by freeze–thaw cycles before use. [D_2]Methylene chloride and [D_5]chlorobenzene were purchased from Armar, stored in Schlenk tubes (Teflon taps) over P_4O_{10}, and distilled and degassed before use. All the chemicals were purchased from Aldrich Chemical Co. or Fluka. Unless otherwise stated, all the reagents were used without further purification. $[Re(NO)_2(PR_3)_2][BAr^F_4]$,[35b] $[Re(OCH\{C_6H_5\})(NO)_2(PR_3)_2][BAr^F_4]$,[35a] and phenyldiazomethane[52] were prepared according to published methods.

Physical measurements: Elemental analyses were performed on a Leco CHNS-932 analyzer at the University of Zurich, Switzerland. ^{1}H, ^{13}C, and ^{31}P{^{1}H} NMR data were recorded on a Bruker Avance DRX500 spectrometer. Chemical shifts are referenced to CD_2Cl_2 or [D_5]chlorobenzene. All chemical shifts for ^{31}P{^{1}H} NMR data are reported downfield relative to external 85% H_3PO_4 at $\delta = 0.0$ ppm. The spectra were processed and analyzed with Bruker XWINNMR software. IR spectra were obtained by the attenuated total reflectance (ATR) method or by using KBr pellets with a Bio-Rad FTS-45 FTIR spectrometer. ESI-MS/MS measurements were performed in a modified Finnigan MAT-TSQ700 mass spectrometer as described in earlier publications.[24]

$[Re(=CH\{C_6H_5\})(NO)_2(PR_3)_2][BAr^F_4]$ with R = Cy (3a) and R = *i*Pr (3b): An excess (~2 equiv) of phenyldiazomethane dissolved in pentane was added to a solution of **2a** (100 mg, 0.06 mmol) or **2b** (100 mg, 0.07 mmol) in benzene (20 mL). The reaction mixture immediately turned from dark red to violet. It was stirred at room temperature for 10 min, then the solvent was removed under reduced pressure. The residue was washed with pentane (3×20 mL) and dried under vacuum. *Compound* ***3a***: yield: 73.6 mg, 70%; ^{1}H NMR (500 MHz, CD_2Cl_2, 25°C): δ = 14.95 (s, 1H, Re[=C*H*{C_6H_5}]), 7.32–7.13 (m, 5H, Re[=CH{C_6H_5}]), 1.82–1.14 (m, 66H, P(C_6H_{11})$_3$); ^{13}C{^{1}H} NMR (125.8 MHz, CD_2Cl_2, 25°C): δ = 271.9 ("t", J_{PC} = 13 Hz, Re(=*C*H{C_6H_5}), 148.8, 134.7, 132.7, 128.4 (s, Re(=CH{*C*$_6$H$_5$}), 35.7 ("t", J_{PC} = 12 Hz, P(*C*$_6$H$_5$)), 29.8, 28.9, 27.3, 27.2, 26.0 (s, P(*C*$_6$H$_5$)); ^{31}P{^{1}H} NMR (121.5 MHz, CD_2Cl_2, 25°C): δ = 19.71 (s, P(C_6H_{11})$_3$); IR (KBr): $\tilde{\nu}$ = 1702, 1631 cm^{-1} (NO); elemental analysis calcd (%) for $C_{75}H_{84}BF_{24}N_2O_2P_2Re$: C 51.13, H 4.81, N 1.59; found: C 51.43; H 4.62, N 1.71.

Compound ***3b***: yield: 95.6 mg, 90%; ^{1}H NMR (500 MHz, CD_2Cl_2, 25°C): δ = 15.04 (s, 1H, Re[=C*H*{C_6H_5}]), 7.67–7.48 (m, 5H, Re[=CH{C_6H_5}]), 2.18 (m, 6H, P{C*H*(CH_3)$_2$}), 1.04 (m, 36H, P{CH(C*H*$_3$)$_2$}); ^{13}C{^{1}H NMR (125.8 MHz, CD_2Cl_2, 25°C): δ = 273.4 ("t", J_{PC} = 13 Hz, Re(=*C*H-{C_6H_5}), 148.2, 135.5, 133.4, 130.4 (s, Re(=CH{*C*$_6$H$_5$}), 26.7 ("t", J_{PC} = 13 Hz, P{*C*H(CH_3)$_2$}), 19.2, 18.4 (s, P{CH(*C*H$_3$)$_2$}); ^{31}P{^{1}H} NMR (121.5 MHz, CD_2Cl_2, 25°C): 29.72 (s, P{CH(CH_3)$_2$}); IR (KBr): $\tilde{\nu}$ = 1697, 1632 cm^{-1} (NO); elemental analysis calcd (%) for $C_{57}H_{69}BF_{24}N_2O_2P_2Re$: C 45.01, H 3.98, N 1.85; found: C 44.79, H 4.05, N 1.88.

$[Re\{CH(C_6H_5)(PR_3)\}(NO)_2(PR_3)][BAr^F_4]$ with R = Cy (23a) and R = *i*Pr (23b): A solution of **3a** (50 mg, 0.03 mmol) or **3b** (50 mg, 0.04 mmol) in chlorobenzene (20 mL) was heated to 60°C and stirred at this temperature for 1 h. It turned from violet to orange. When the reaction was complete, the solvent was removed under reduced pressure. The residue was washed with pentane (3×20 mL) and dried under reduced pressure.

Compound ***23a***: yield: 48.1 mg, 95%; ^{1}H NMR (500 MHz, CD_2Cl_2, 25°C): δ = 7.26–7.17 (m, 5H, Re{CH(C_6H_5)[P(C_6H_{11})$_3$]}), 3.42 (br s, 1H, Re{C*H*(C_6H_5)[P(C_6H_{11})$_3$]}), 2.19–1.77 (m, 66H, Re{CH(C_6H_5)[P(C_6H_{11})$_3$]} and P(C_6H_{11})$_3$); ^{13}C{^{1}H} NMR (125.8 MHz, CD_2Cl_2, 25°C): δ = 135.1, 129.2, 123.8, 121.6 (s, Re{CH(*C*$_6$H$_5$)[P(C_6H_{11})]}), 34.8 (d, J_{PC} = 24 Hz, P(*C*$_6$H$_{11}$)$_3$), 33.2 (d, J_{PC} = 40 Hz, Re{CH(C_6H_5)[P(*C*$_6$H$_{11}$)]}), 29.6 (br s, {CH(C_6H_5)[P(*C*$_6$H$_{11}$)$_3$]}), 29.5 (s, P(*C*$_6$H$_{11}$)$_3$), 27.6 (s, P(*C*$_6$H$_{11}$)$_3$), 27.3 (br s, {CH(C_6H_5)[P(*C*$_6$H$_{11}$)$_3$]}), 26.0 (br s, {CH(C_6H_5)[P(*C*$_6$H$_{11}$)$_3$]}), 25.5 (s, P(*C*$_6$H$_{11}$)$_3$), 20.8, 21.1 (br d, J_{PC} = 20 Hz, Re{*C*H(C_6H_5)[P(C_6H_{11})]}); ^{31}P{^{1}H} NMR (121.5 MHz, CD_2Cl_2, 25°C): δ = 40.32, 40.41 (2 s, Re-{CH(C_6H_5)[*P*(C_6H_{11})$_3$]}), 27.02 (s, *P*(C_6H_{11})$_3$). The assignment of the ^{1}H NMR and ^{13}C{^{1}H} NMR signals was confirmed by ^{13}C DEPT, HMQC, HSQC, and COSY experiments. IR (ATR): $\tilde{\nu}$ = 1643, 1583 cm^{-1} (NO); elemental analysis calcd (%) for $C_{75}H_{84}BF_{24}N_2O_2P_2Re$: C 51.13, H 4.81, N 1.59; found: C 51.42, H 4.53, N 1.65.

Compound ***23b***: yield: 48.1 mg, 96%; ^{1}H NMR (500 MHz, CD_2Cl_2, 25°C): δ = 7.56–7.29 (m, 5H, Re{CH(C_6H_5){P[CH(CH_3)$_2$]$_3$}}), 3.75 (br s, 1H, Re{C*H*(C_6H_5)[P[CH(CH_3)$_2$]$_3$]}), 2.68, 2.02 (m, 6H, P{C*H*(CH_3)$_2$}$_3$), 1.52–1.02 (m, 36H, P{CH(C*H*$_3$)$_2$}$_3$); ^{13}C{^{1}H} NMR (125.8 MHz, CD_2Cl_2, 25°C): δ = 134.28, 132.21, 131.71, 130.49 (s, Re{CH(C_6H_5)-{P[CH(CH_3)$_2$]$_3$}}), 25.32 (d, J_{PC} = 25 Hz, {P[*C*H(CH_3)$_2$]$_3$}), 23.64 (d, J_{PC} = 40 Hz, Re{CH(C_6H_5){P[*C*H(CH_3)$_2$]$_3$}}), 21.83, 21.71 (2 d, J_{PC} = 23 Hz, Re{*C*H(C_6H_5){P[CH(CH_3)$_2$]$_3$}}), 19.94 (d, J_{PC} = 18 Hz, {P[CH(*C*H$_3$)$_2$]$_3$}), 19.44, 19.39 (2 d, J_{PC} = 20 Hz, Re{CH(C_6H_5){P[CH(*C*H$_3$)$_2$]$_3$}}); ^{31}P{^{1}H} NMR (121.5 MHz, CD_2Cl_2, 25°C): δ = 50.87 (br s, Re{CH(C_6H_5)-[P[CH(*C*H$_3$)$_2$]$_3$]}), 44.92 (s, P{CH(*C*H$_3$)$_2$}$_3$). The assignments of the ^{1}H NMR and ^{13}C{^{1}H} NMR signals were confirmed by ^{13}C DEPT, HMQC, HSQC, and COSY experiments. IR (ATR): $\tilde{\nu}$ = 1655, 1609 cm^{-1} (NO); elemental analysis calcd (%) for $C_{57}H_{60}BF_{24}N_2O_2P_2Re$: C 45.01, H 3.98, N 1.85; found: C 45.39, H 3.99, N 1.91.

ROMP reactions: In a typical ROMP experiment, catalyst (0.002 mmol) was dissolved in chlorobenzene (0.5 mL) and added to a chlorobenzene solution (0.5 mL) of the appropriate olefin (1.3 mmol). The reaction mixtures became viscous after several minutes, indicating polymer formation. After reaction for 1 h the mixtures were poured into MeOH (100 mL), resulting in precipitation of the white polymers. The polymers were collected and washed with MeOH (2×20 mL), dried under reduced pressure, and characterized by various NMR techniques and GPC measurements.

X-ray structure analysis of 3a and 23a: Crystals of **3a** and **23a**, protected in hydrocarbon oil, were selected for the X-ray experiments using a polarizing microscope. They were mounted on the tip of a glass fiber and immediately transferred to the goniometer of an imaging plate detector system (Stoe IPDS diffractometer), where they were cooled to 183(2) K in an Oxford Cryogenic System. The crystal-to-image distances were set to 50 mm for both compounds (λ_{max} = 30.31 and 30.41°). The φ oscillation scan modes were applied according to the relatively low diffraction power of the crystals being measured. For the cell parameter refinements 7997 and 8000 reflections were selected out of the whole limiting spheres. A total of 48061 (**3a**) and 57842 (**23a**) diffraction intensities were collected,[53] of which 21087 (**3a**) and 22098 (**23a**) were unique (R_{int} = 0.0641 and 0.0746) after data reduction. Numerical absorption corrections[54] based on 16 and 10 crystal faces were applied with FACEitVIDEO and XRED.[53] The structures were solved by the Patterson method using the SHELXS-97 program.[55] Interpretation of the difference Fourier maps, preliminary plot generation, and checking for higher symmetry were performed with PLATON[56] and the LEPAGE program.[57] All heavy atoms were refined (SHELXL-97)[58] using anisotropic displacement parameters. Positions of H-atoms were calculated after each refinement cycle (riding model). Structural plots (Figures 1 and 3) were generated using ORTEP.[59]

CCDC-244439 and -244440 contain the supplementary crystallographic data for this paper. These data can be obtained free of charge from the CambridgeCrystallographic Data Centre via www.ccdc.cam.ac.uk/data_request/cif

Computational details: Density functional theory (DFT) calculations were performed with the TURBOMOLE program package, version 5.5.[60] The Vosko–Wilk–Nusair[61] local density approximation (LDA) and the generalized gradient approximation (GGA) with corrections for exchange and correlation according to Becke[62] and Perdew[63] (BP86) were used for all calculations. The TURBOMOLE approach to DFT GGA calculations is based on the use of Gaussian-type orbitals (GTO) as basis functions. Geometries were optimized within the framework of the RI-*J* approximation[64] using accurate triple-ζ valence basis sets augmented by one polarization function TZV(P)[65] for all elements. The effective core potential (ECP) was employed to model the energetically deep-lying and chemically mostly inert relativistic 60 core electrons of the rhenium atom. The geometry optimizations, managed mainly through the use of the RIDFT, RDGRAD and RELAX modules supplied with the TURBOMOLE program package, were considered converged after the change in total energy was less than 10^{-6} Hartrees and the norm of the Cartesian gradient was smaller than 10^{-3} Hartrees Å^{-1} (or 3×10^{-2} Hartrees Å^{-1} for constrained geometry optimizations).

Acknowledgements

We thank CIBA Specialty Chemicals Inc. (Basel) for analysis of the polymers produced. This work is supported by the Swiss National Science Foundation (SNSF).

[1] K. J. Ivin, J. C. Mol in *Olefin Metathesis and Metathesis Polymerization* (Eds.: K. J. Ivin, J. C. Mol), Academic Press, San Diego, **1997**.
[2] F. Zaragoza Dörwald in *Metal Carbenes in Organic Synthesis*, Wiley-VCH, Weinheim, **1999**.
[3] A. Fürstner, *Angew. Chem.* **2000**, *112*, 3140; *Angew. Chem. Int. Ed.* **2000**, *39*, 3012.
[4] T. M. Trnka, R. H. Grubbs, *Acc. Chem. Res.* **2001**, *34*, 18.
[5] a) H. S. Eleuterio, US Patent 3074918, **1963**; b) H. S. Eleuterio, *J. Mol. Catal.* **1991**, *65*, 55; c) there is earlier evidence for the discovery of the metathesis reaction in polymer chemistry (ROMP): A. W. Anderson, N. G. Merckling, US Patent 2721189, **1955**; d) for a comprehensive review: K. J. Ivin, J. C. Mol in *Olefin Metathesis and Metathesis Polymerization* (Eds.: K. J. Ivin, J. C. Mol), Academic Press, San Diego, **1997**.
[6] N. Calderon, H. Y. Chen, R. W. Scott, *Tetrahedron Lett.* **1967**, *8*, 3327.
[7] S. T. Nguyen, L. K. Johnson, R. H. Grubbs, J. W. Ziller, *J. Am. Chem. Soc.* **1992**, *114*, 3974.
[8] A. Demonceau, A. F. Noels, E. Saive, A. J. Hubert, *J. Mol. Catal.* **1992**, *76*, 123.
[9] P. Schwab, R. H. Grubbs, J. W. Ziller, *J. Am. Chem. Soc.* **1996**, *118*, 100.
[10] a) S. M. Hansen, F. Rominger, M. Metz, P. Hofmann, *Chem. Eur. J.* **1999**, *5*, 557; b) S. M. Hansen, M. A. O. Volland, F. Rominger, F. Eisenträger, P. Hofmann, *Angew. Chem.* **1999**, *111*, 1360; *Angew. Chem. Int. Ed.* **1999**, *38*, 1273; c) P. Hofmann, M. A. O. Volland, S. M. Hansen, F. Eisenträger, J. H. Gross, K. Stengel, *J. Organomet. Chem.* **2000**, *606*, 88.
[11] a) M. Scholl, T. M. Trnka, J. P. Morgan, R. H. Grubbs, *Tetrahedron Lett.* **1999**, *40*, 2247; b) M. Scholl, S. Ding, W. C. Lee, R. H. Grubbs, *Org. Lett.* **1999**, *1*, 953.
[12] a) J. Huang, E. D. Stevens, S. P. Nolan, J. L. Petersen, *J. Am. Chem. Soc.* **1999**, *121*, 2674; b) J. Huang, H.-J. Schanz, S. P. Nolan, *Organometallics* **1999**, *18*, 5375.
[13] a) T. Weskamp, F. J. Kohl, W. Hieringer, D. Gleich, W. A. Herrmann, *Angew. Chem.* **1999**, *111*, 2573; *Angew. Chem. Int. Ed.* **1999**, *38*, 2416; b) L. Ackermann, A. Fürstner, T. Weskamp, F. J. Kohl, W. A. Herrmann, *Tetrahedron Lett.* **1999**, *40*, 4787; c) T. Weskamp, F. J. Kohl, W. A. Herrmann, *J. Organomet. Chem.* **1999**, *582*, 362.
[14] Reviews of NHC: a) W. A. Herrmann, C. Köher, *Angew. Chem.* **1997**, *109*, 2256; *Angew. Chem. Int. Ed.* **1997**, *36*, 2162; b) A. J. Arduengo, *Acc. Chem. Res.* **1999**, *32*, 913.
[15] R. H. Grubbs, S. J. Miller, G. C. Fu, *Acc. Chem. Res.* **1995**, *28*, 446.
[16] a) R. R. Schrock, J. S. Murdzek, G. C. Bazan, J. Robbins, J. Dimare, M. B. O'Regan, *J. Am. Chem. Soc.* **1990**, *112*, 3875; b) G. C. Bazan, E. Khosravi, R. R. Schrock, W. J. Feast, V. C. Gibson, M. B. O'Regan, J. K. Thomas, W. M. Davis, *J. Am. Chem. Soc.* **1990**, *112*, 8378; c) G. C. Bazan, H. Oskam, H. N. Cho, L. Y. Park, R. R. Schrock, *J. Am. Chem. Soc.* **1991**, *113*, 6899.
[17] P. E. Romero, W. E. Piers, R. McDonald, *Angew. Chem.* **2004**, *116*, 6287; *Angew. Chem. Int. Ed.* **2004**, *43*, 6161.
[18] E. L. Dias, S. T. Nguyen, R. H. Grubbs, *J. Am. Chem. Soc.* **1997**, *119*, 3887.
[19] M. Ulman, R. H. Grubbs, *Organometallics* **1998**, *17*, 2484.
[20] M. Ulman, R. H. Grubbs, *J. Org. Chem.* **1999**, *64*, 7202.
[21] M. S. Sanford, M. Ulman, R. H. Grubbs, *J. Am. Chem. Soc.* **2001**, *123*, 749.
[22] M. S. Sanford, J. A. Love, R. H. Grubbs, *J. Am. Chem. Soc.* **2001**, *123*, 6543.
[23] C. Hinderling, C. Adlhart, P. Chen, *Angew. Chem.* **1998**, *110*, 2831; *Angew. Chem. Int. Ed.* **1998**, *37*, 2685.
[24] C. Adlhart, C. Hinderling, H. Baumann, P. Chen, *J. Am. Chem. Soc.* **2000**, *122*, 8204.
[25] C. Adlhart, M. A. O. Volland, P. Hofmann, P. Chen, *Helv. Chim. Acta* **2000**, *83*, 3306.
[26] M. A. O. Volland, C. Adlhart, C. A. Kiener, P. Chen, P. Hofmann, *Chem. Eur. J.* **2001**, *7*, 4621.
[27] J. A. Tallarico, P. J. Bonitatebus Jr., M. L. Snapper, *J. Am. Chem. Soc.* **1997**, *119*, 7157.
[28] M. S. Sanford, L. M. Henling, M. W. Day, R. H. Grubbs, *Angew. Chem.* **2000**, *112*, 3593; *Angew. Chem. Int. Ed.* **2000**, *39*, 3451.
[29] M. T. Reetz, M. H. Becker, M. Liebl, A. Fürstner, *Angew. Chem.* **2000**, *112*, 1294; *Angew. Chem. Int. Ed.* **2000**, *39*, 1236.
[30] A. Fürstner, L. Ackermann, B. Gabor, R. Goddard, C. W. Lehmann, R. Mynott, F. Stelzer, O. R. Thiel, *Chem. Eur. J.* **2001**, *7*, 3236.
[31] a) E. J. Howman, L. Turner, Dutch Patent 6605328, **1966**; b) J. Cosyns, J. Chodorge, D. Commereuc, B. Torck, *Hydrocarbon Process.* **1998**, 60.
[32] X. Chen, X. Zhang, P. Chen, *Angew. Chem.* **2003**, *115*, 3928; *Angew. Chem. Int. Ed.* **2003**, *42*, 3798.
[33] a) W. A. Herrmann, *J. Organomet. Chem.* **1995**, *500*, 149; b) C. C. Romao, F. E. Kühn, W. A. Herrmann, *Chem. Rev.* **1997**, *97*, 3197; c) R. R. Schrock, R. T. Depue, J. Feldman, C. J. Schaverien, J. C.

Dewan, A. H. Liu, *J. Am. Chem. Soc.* **1988**, *110*, 1423; d) M. H. Schofield, R. R. Schrock, L. Y. Park, *Organometallics* **1991**, *10*, 1844; e) A. Weinstock, R. R. Schrock, W. M. Davis, *J. Am. Chem. Soc.* **1991**, *113*, 135; f) R. Toreki, R. R. Schrock, *J. Am. Chem. Soc.* **1990**, *112*, 2448; g) R. Toreki, R. R. Schrock, *J. Am. Chem. Soc.* **1992**, *114*, 3367; h) R. Toreki, G. A. Vaughan, R. R. Schrock, W. M. Davis, *J. Am. Chem. Soc.* **1993**, *115*, 127; i) R. Toreki, R. R. Schrock, W. M. Davis, *J. Organomet. Chem.* **1996**, *520*, 69; j) G. A. Vaughan, R. Toreki, R. R. Schrock, W. M. Davis, *J. Am. Chem. Soc.* **1993**, *115*, 2980; k) A. M. LaPointe, R. R. Schrock, *Organometallics* **1995**, *14*, 1875.

[34] a) T. J. Katz, N. Acton, *Tetrahedron Lett.* **1976**, *17*, 4251; b) M. Doherty, A. Siove, A. Parlier, H. Rudler, M. Fontanille, *Makromol. Chem. Macromol. Symp.* **1986**, *6*, 33; c) S. Warwel, V. Siekermann, *Makromol. Chem. Rapid Comm.* **1983**, *4*, 423.

[35] a) H. Jacobsen, K. Heinze, A. Llamazares, H. W. Schmalle, G. Artus, H. Berke, *J. Chem. Soc. Dalton Trans.* **1999**, 1717; b) A. Llamazares, H. W. Schmalle, H. Berke, *Organometallics* **2001**, *20*, 5277; c) D. G. Gusev, A. Llamazares, G. Artus, H. Jacobsen, H. Berke, *Organometallics* **1999**, *18*, 75.

[36] a) E. A. Zuech, *Chem. Commun.* **1968**, 1182; b) E. A. Zuech, W. B. Hughes, D. H. Kubicek, E. T. Kittleman, *J. Am. Chem. Soc.* **1970**, *92*, 528; c) R. Taube, K. Z. Seyferth, *Chem. Br.* **1977**, *13*, 300; d) R. Taube, K. Seyferth, *Z. Anorg. Allg. Chem.* **1973**, *437*, 213; e) M. Leconte, J.-M. Basset, *J. Am. Chem. Soc.* **1979**, *101*, 7296; f) K. Seyferth, K. Rosenthal, G. Kühn, R. Taube, *Z. Anorg. Allg. Chem.* **1984**, *513*, 57; g) K. Seyferth, R. Taube, *J. Organomet. Chem.* **1984**, *262*, 191; h) A. Keller, L. Szterenberg, *J. Mol. Catal.* **1989**, *57*, 207; i) A. Keller, *J. Organomet. Chem.* **1990**, *407*, 237; j) A. Keller, L. Szterenberg, *Z. Naturforsch. Teil B* **1991**, *47*, 1469; k) A. Keller, *J. Organomet. Chem.* **1992**, *436*, 199; l) A. Keller, *J. Mol. Catal.* **1993**, *78*, L15; m) A. Keller, R. Matusiak, *J. Mol. Catal. A* **1996**, *104*, 213; n) A. Keller, J. M. Sobczak, R. Matusiak, *J. Mol. Catal. A* **1998**, *136*, 115; o) A. Keller, R. Matusiak, *J. Mol. Catal. A* **1999**, *142*, 317; p) R. Matusiak, A. Keller, *Polym. Bull.* **1999**, *43*, 199.

[37] a) W. Beck, A. Melnikoff, R. Stahl, *Chem. Ber.* **1966**, *99*, 3721; b) A. Poletti, A. Foffani, R. Cataliotti, *Spectrochim. Acta* **1970**, *26A*, 1063.

[38] a) J. M. E. Matos, B. S. Lima-Neto, *J. Mol. Catal. A* **2004**, *222*, 81; b) N. Cobo, M. A. Esteruelas, F. Gonzalez, J. Herrero, A. M. Lopez, P. Lucio, M. Olivan, *J. Catal.* **2004**, *223*, 319; c) L. Bencze, N. Biro, B. Szabo-Ravasz, L. Mihichuk, *Can. J. Chem.* **2004**, *82*, 499.

[39] a) K. J. Ivin, B. S. R. Reddy, J. J. Rooney, *J. Chem. Soc. Chem. Commun.* **1981**, 1062; b) G. J. Spivak, J. N. Coalter, *Organometallics* **1998**, *17*, 999; c) J. N. Coalter, G. J. Spivak, H. Gérard, E. Clot, E. R. Davidson, O. Eisenstein, K. C. Caulton, *J. Am. Chem. Soc.* **1998**, *120*, 9388; d) J. N. Coalter, J. C. Bollinger, O. Eisenstein, K. G. Caulton, *New J. Chem.* **2000**, *24*, 925; e) G. Ferrando-Miguel, J. N. Coalter, H. Gerard, J. C. Huffman, O. Eisenstein, K. G. Caulton, *New J. Chem.* **2002**, *26*, 687; f) G. Ferrando, H. Gerard, G. J. Spivak, J. N. Coalter, J. C. Huffman, O. Eisenstein, K. G. Caulton, *Inorg. Chem.* **2001**, *40*, 6610; g) J. N. Coalter, J. C. Bollinger, J. C. Huffman, U. Werner-Zwanziger, K. G. Caulton, E. R. Davidson, E. Clot, O. Eisenstein, *New J. Chem.* **2000**, *24*, 9; h) N. Dolker, G. Frenking, *J. Organomet. Chem.* **2001**, *617*, 225.

[40] a) O. Dereli, B. Düz, B. Zümreoglu-Karan, Y. Imanoglu, *Appl. Organomet. Chem.* **2004**, *18*, 130; b) Y. Nakayama, K. Katsuda, H. Yasuda, *Polym. J.* **2003**, *35*, 896; c) E. P. Bokaris, M. M. Kosmas, *J. Mol. Catal. A* **2003**, *192*, 263; d) S. Hayano, H. Kurakata, Y. Tsunogae, Y. Nakayama, Y. Sato, H. Yasuda, *Macromolecules* **2003**, *36*, 7422.

[41] a) S. M. Hansen, F. Rominger, M. Metz, P. Hofmann, *Chem. Eur. J.* **1999**, *5*, 557.

[42] When the metal center is released from the polymer after treatment of the reaction mixture with methanol, the following liberation mechanism can be envisaged (see also the later text). After coordination of methanol with the metal center, protonation of the iminate unit might occur, accompanied by its dissociation and formation of a rhenium–alkoxy complex. Because of the poor electron acceptor nature of the carbene ligand, methanol might attack the $C_{carbene}$ nucleophilically, resulting in the formation of an alkyl unit, which could be labile, bonded to the metal center. If dissociation occurs, immediate protonation of the alkyl unit and liberation of the polymer chain would be accompanied by formation of an alkoxy–rhenium species. However, no experimental evidence has been obtained, nor theoretical investigation performed, which could support the proposed polymer liberation mechanism.

[43] The basic electrospray source for mass spectrometry is described by: C. M. Whitehouse, R. N. Dreyer, M. M. Yamashita, J. B. Fenn, *Anal. Chem.* **1985**, *57*, 675.

[44] A complete monograph on the technique is: *Electrospray Ionization Mass Spectrometry* (Ed.: R. D. Cole), Wiley, New York, **1997**.

[45] a) C. Adlhart, C. Hinderling, H. Baumann, P. Chen, *J. Am. Chem. Soc.* **2000**, *122*, 8204; b) C. Hinderling, C. Adlhart, P. Chen, *Angew. Chem.* **1998**, *110*, 2831; *Angew. Chem. Int. Ed.* **1998**, *37*, 2685.

[46] M. A. O. Volland, C. Adlhart, C. A. Kiener, P. Chen, P. Hofmann, *Chem. Eur. J.* **2001**, *7*, 4621.

[47] T. T. Cuc, T. Bastelberger, H. Höcker, *J. Mol. Catal.* **1985**, *28*, 279.

[48] a) H. Katayama, H. Urushima, F. Ozawa, *J. Organomet. Chem.* **2000**, *606*, 16; b) P. A. van der Schaaf, R. Kolly, H. J. Kirner, F. Rime, A. Muhlebach, A. Hafner, *J. Organomet. Chem.* **2000**, *606*, 65.

[49] C. Adlhart, Ph.D. Thesis, ETH Zürich, **2003**.

[50] M. S. Sanford, J. A. Love, R. H. Grubbs, *J. Am. Chem. Soc.* **2001**, *123*, 6543.

[51] M. J. Szabo, H. Berke, T. Weiss, T. Ziegler, *Organometallics* **2003**, *22*, 3671.

[52] X. Creary, *Synthesis* **1986**, 207.

[53] Stoe IPDS software for data collection, cell refinement, and data reduction, Version 2.92, Stoe & Cie GmbH, Darmstadt, Germany, **1999**.

[54] P. Coppens, L. Leiserowitz, D. Rabinovich, *Acta Crystallogr.* **1965**, *18*(6), 1035.

[55] G. M. Sheldrick, *Acta Crystallogr.* Sect. *A* **1990**, 46, 467.

[56] A. L. Spek, *Acta Crystallogr. Sect. A* **1990**, *46*, C34.

[57] Y. Le Page, *J. Appl. Crystallogr.* **1987**, *20*, 264.

[58] G. M. Sheldrick, SHELXL-97: Software package for crystal structure determination and refinement, University of Göttingen, Göttingen, Germany, **1997**.

[59] C. K. Johnson, ORTEPII, Report ORNL-5138, Oak Ridge National Laboratory, Oak Ridge (TN), **1976**.

[60] TURBOMOLE, Program package for ab initio electronic structure calculations, Theoretical Chemistry Groups, University of Karlsruhe, Germany; http://www.turbomole.com; a) R. Ahlrichs, M. Bär, M. Häser, H. Horn, C. Kölmel, *Chem. Phys. Lett.* **1989**, *162*, 165; b) O. Treutler, R. Ahlrichs, *J. Chem. Phys.* 1995, ***102***, 346; c) M. von Arnim, R. Ahlrichs, *J. Comput. Chem.* **1998**, *19*, 1746.

[61] S. H. Vosko, L. Wilk, M. Nusair, *Can. J. Phys.* **1980**, *58*, 1200.

[62] A. D. Becke, *Phys. Rev. A* **1988**, *38*, 3098.

[63] a) J. P. Perdew, *Phys. Rev. B* **1986**, *33*, 8822; b) J. P. Perdew, *Phys. Rev. B* **1986**, *34*, 7406.

[64] a) K. Eichkorn, O. Treutler, H. Öhm, M. Häser, R. Ahlrichs, *Chem. Phys. Lett.* **1995**, *240*, 283; b) K. Eichkorn, O. Treutler, H. Öhm, M. Häser, R. Ahlrichs, *Chem. Phys. Lett.* **1995**, *242*, 652; c) K. Eichkorn, F. Weigand, O. Treutler, R. Ahlrichs, *Theor. Chem. Acc.* **1997**, *97*, 119.

[65] A. Schäfer, C. Huber, R. Ahlrichs, *J. Chem. Phys.* **1994**, *100*, 5829.

Received: August 22, 2005
Published online: February 3, 2006

